MVA'90 IAPR Workshop on Machine Vision Applications Nov. 28-30,1990, Tokyo

Application of Image Reconstruction by Means of Chirp z-Transform

Kunio Takaya, Tie-nan Ma
Koichi Shimizu*, Masataka Kitama*, Tomohisa Mikami*

Elec. Eng. University of Saskatchewan, Saskatoon, Canada
*** Bio. Med. Eng. Hokkaido University, Sapporo, Japan**

Abstract

The optical CT (Computerized Tomography), which utilises light transmitted through a semi-opaque object extends vision to the inside of objects. The projection profiles of the optical CT are smeared due to the scattering of light in a translucent medium. In the image reconstruction for MRI (Magnetic Resonance Imaging), FID (Free Induction Decay) signals consisting of decaying sinusoids inevitably produce smeared spectra. The chirp-z transform provides an effective means which reduces such smearing, when the DFT (Discrete Fourier Transform) used in different stages of image reconstruction processes, is replaced by the CZT (Chirp z-Transform). This paper discusses the peak value and the bandwidth of the improved spectrum by CZT in relation to the ordinary DFT (Discrete Fourier Transform) method and proper selection of a contour for a given set of data. The validity of replacing DFT by CZT in different image reconstruction schemes is also discussed. The improvement in image quality is demonstrated for the experimental data obtained from an optical CT system and that obtained from MRI specifically for the purpose of chemical-shift imaging.

The Chirp z-Transform

DFT evaluates z-transforms on the unit circle in the z-plane, whereas the chirp z-transform evaluates them on a spiral contour inside or outside the unit circle. Since one can adjust the contour such that the contour passes through or comes close to the poles of a signal under study, the spectrum is sharpened, and its frequency resolution is appreciably improved.

When a sequence of N data x_n, $n = 0...N-1$ is sampled from an analog signal, the z-transform of this finite sequence is given by

$$X(z) = \sum_{n=0}^{N-1} x_n z^{-n}. \qquad (1)$$

When $X(z)$ is evaluated at

$$z_k = e^{j\frac{2\pi}{N}k}, \quad k = 0 \ldots N-1 \qquad (2)$$

in the complex plane, $X(z_k), k = 0 \ldots N-1$ is the DFT of x_n. When z-transform is evaluated at

$$z_k = A\,W^{-r} \qquad (3)$$

for arbitrary complex numbers, $A = A_0 e^{j\theta_0}$ and $W = W_0 e^{-j\phi_0}$, $X(z_k)$ is referred to as the chirp z-transform of x_n. In CZT, the contour used in evaluating $X(z)$ is changed from the unit circle in DFT to a segment of the arc which spirals in or out relative to the unit circle. A simple exponentially decaying sinusoidal signal is represented by two poles located at $r\,e^{\pm j\theta}$. The k-th discrete spectrum $X(z_k)$ is inversely proportional to the distance between each of the poles and z_k, since

$$X(z_k) = \frac{1}{(z - r\,e^{j\theta})(z - r\,e^{-j\theta})}\Big|_{z=z_k}. \qquad (4)$$

This means that the discrete spectrum evaluated along the arc passing through or close to the poles of a given signal exhibits sharper spectrum than those determined by DFT using a fixed contour of the unit circle.

Consider the discrete sequence of data sampled from a decaying sinusoidal wave,

$$x(n) = e^{j\frac{2\pi k}{N}n\Delta}\, e^{\frac{-n\Delta}{T}} \quad n = 0 \ldots N-1. \qquad (5)$$

Δ is a sampling interval and T is the time constant of decay. It is assumed that the frequency of sinusoidal oscillation f_k satisfies $k = f_k N\Delta$ being an integer. Discrete spectral analysis can be applied to Eq. 5. If the spectrum $X(z_k)$ representing the frequency f_k is calculated by using the z_k defined in Eq. 2, the result is of DFT. On the other hand, if Eq. 3 is used, the spectrum is of CZT. Two important indecies in spectral analysis, peak height and peak width (defined by half-power points) of spectral lines are theoretically studied and are presented elsewhere in detail [2]. The peak height and width for DFT denoted by $|X(z_k)|$ and Δf respectively, and $|X_c(z_k)|$ and Δf_c for CZT are given as follows:

$$\lim_{T\to\infty} |X(z_k)| = N \qquad (6)$$

$$\Delta f = \frac{1}{\pi T} \tag{7}$$

$$|X_c(z_k)| = N \tag{8}$$

$$\Delta f_c \simeq const. \tag{9}$$

The inequalities that $|X(z_k)| < |X_c(z_k)|$ and $\Delta f > \Delta f_c$ are satisfied for a relatively small T.

Applications of CZT to Imaging

Chemical-shift Imaging in MRI

Chemical-shift imaging is the 2- or 3- dimensional NMR spectroscopy carried out noninvasively for the inside a human body. Results can be displayed either in the form of NMR spectrum at a selected point or as a 2- or 3-dimensional map representing a specific chemical species or structure.[1] The NMR signal called FID signal obtained as a RF (Radio Frequency) echo of magnetic resonance is used as raw data for image reconstruction. In addition to the static magnetic field, gradient fields are superimposed for a short time ΔT to attach positional information to FID signals by phase encoding. The FID signal originating from a point source $\rho(x, y)$ is given by

$$s(x, y, \omega, t) = \rho(x, y) e^{j\gamma(G_x x + G_y y)\Delta T} e^{j\omega t} e^{\frac{-t}{T_2^*}} \tag{10}$$

The actual measured signal is the integration of Eq. 10 over the three variables, x, y and ω. Measurements are repeated for different levels of gradient fields G_x and G_y as follows.

$$G_x = \Delta G_x(\ell - M/2), \quad \ell = 0, 1, \ ..., \ M-1 \tag{11}$$

$$G_y = \Delta G_y(m - M/2), \quad m = 0, 1, \ ..., \ M-1 \tag{12}$$

Introducing discrete variables n, i and j satisfying $t = n\Delta$, $x = \Delta x i$, and $y = \Delta y j$ and also ignoring the exponential decay, the signal from the point source is expressed in terms of ℓ, m and n.

$$\begin{aligned} s(\ell, m, n) =& \rho(x, y) e^{j\gamma \Delta G_x (\ell - M/2)\Delta x i \Delta T} \\ & e^{j\gamma \Delta G_y (m - M/2)\Delta y j \Delta T} e^{j\omega n \Delta} \end{aligned} \tag{13}$$

Applying proper scaling for gradient field intensities and the duration ΔT,

$$\gamma \Delta G_x \Delta x \Delta T = 2\pi/M, \qquad \Delta x M = x_{max} \tag{14}$$

$$\gamma \Delta G_y \Delta y \Delta T = 2\pi/M, \qquad \Delta y M = y_{max} \tag{15}$$

The 3-dimensional DFT of $s(\ell, m, n)$ yields the general principle of image reconstruction necessary for chemical-shift imaging.

$$\begin{aligned} \mathcal{F}[s(\ell, m, n)] = & M^2 N \rho(i, j)(-1)^{i+j} \\ & \delta(i - p)\delta(j - q)\delta(r - \frac{\omega \Delta N}{2\pi}) \end{aligned} \tag{16}$$

The DFT with respect to time affects the term $e^{j\omega t} e^{\frac{-t}{T_2^*}}$ in Eq. 10, in which ω is chemical-shift frequency and T_2^* is a spin-spin relaxation time of FID signals. As this part forms a pair of complex poles, spectral sharpening is be expected, if this DFT is replaced by the CZT.

Filtered Back-projection in Optical CT

When the internal structure of a translucent object is to be optically determined by tomographic techniques, the same image reconstruction algorithm as used in X-ray CT is applicable. Opaque objects are often transparent to the extent that the information of inside structure is detectable. However, scattering occurring along the path of light usually obscures the image of the source. In order to make such objects visible, the component of scattering light included in the light transmitted through media must be suppressed. The use of a collimator lens, which prevents scattered light from reaching the detector, is an effective means.

In 2-dimensional optical CT, an object is projected towards a line perpendicular to the parallel rays of incident light. The profile of a projection $p(t, \theta)$ is the intensity of the light passing through the object, at a beam position t and a given angle θ. When the transmittance of a 2-dimensional object at a Cartesian coordinate of (x, y) is given by $f(x, y)$, the projection is,

$$p(t, \theta) = \int_L f(x, y) d\ell, \tag{17}$$

where the line L is defined by $\ell = x\cos\theta + y\sin\theta$. Let $F(u, v) = \mathcal{F}[f(x, y)]$, 2-dimensional Fourier transform of $f(x, y)$. Image reconstruction projections heavily relies on the theorem:

$$\begin{aligned} P(\omega, \theta) &= \int_{-\infty}^{\infty} p(t, \theta) e^{-i\omega t} dt \\ &= F(\omega\cos\theta, \omega\sin\theta). \end{aligned} \tag{18}$$

The Fourier transform of a projection $p(t, \theta)$ is the axial cross-section of the 2-dimensional Fourier transform of the object $f(x, y)$. Thus, the original image can be reconstructed by taking the inverse Fourier transform of $F(u, v)$, or by utilizing the following relationship:

$$\begin{aligned} f(x, y) = & \frac{1}{4\pi^2} \times \\ & \int_0^{\pi} d\theta \int_{-\infty}^{\infty} P(\omega, \theta) e^{i\omega(x\cos\theta + y\sin\theta)} |\omega| \, d\omega. \end{aligned} \tag{19}$$

The second integration means the inverse Fourier transform of $P(\omega, \theta)|\omega|$. Since all points in the

(x, y) plane satisfying $t = x\cos\theta + y\sin\theta$ take the same value, the inverse Fourier transform

$$p_0(t,\theta) = \int_{-\infty}^{\infty} P(\omega,\theta) e^{i\omega t} |\omega| \, d\omega \qquad (20)$$

must be back-projected to reconstruct the image $f(x, y)$. The function $p_0(t, \theta)$ can be calculated either by Eq. 20 in the Fourier domain or by the convolution in time domain using $\mathcal{F}^{-1}\,|\omega|$.

The projection $p(t, \theta)$ given by Eq. 17 is nothing more than a conceptual definition. There is an implicit assumption in this equation that the projection by a single beam placed at $t = t_0$ has a point spread function given by

$$p_s(t,\theta) = \delta(t - t_0). \qquad (21)$$

However, the point spread function in reality is closely approximated by a Gaussian function,

$$p_s(t,\theta) = K\, e^{-a(t-t_0)^2}, \qquad (22)$$

because the scattering light has a cosine radiation pattern, and also obeys the r^{-2} rule (r: distance) diminishing the scattered light from far fields rapidly as t moves away from t_0. When medium is not clear but translucent, the point spread function do not decay as rapidly as the Gaussian function. It exhibits a long slowly decaying tail, instead. A better approximation of the point spread function is

$$p_s(t,\theta) = \frac{K}{a^2 + (t - t_0)^2}. \qquad (23)$$

Since the actual projection affected by the point spread function is given by convolution $p(t, \theta) * p_s(t, \theta)$, $P(\omega, \theta)$ in Eq. 19 is replaced by $P(\omega, \theta)\, P_s(\omega, \theta)$. The Fourier transform of Eq. 23 is

$$P_s(\omega,\theta) = e^{-a|\omega|}. \qquad (24)$$

In order to compensate the effect of the point spread function, the inverse of Eq. 24 should be included in Eq. 20, which means that the CZT applied to $P(\omega, \theta)|\omega|$ produces the function $p_0(t, \theta)$ to be back projected for image reconstruction. The $p_0(t, \theta)$ is filtered for high emphasis and compensated for the point spread function. As Eq. 20 is the inverse Fourier transform, the rotation of the spiraling contour of the CZT must therefore be reversed.

Experimental Results

The proposed method of sharpening spectral peaks by the CZT is applied to a phantom consisting of five glass tubes, in which three are filled with methanol (CH_3-OH) and the remaining two are filled with ethanol (CH_3-CH_2-OH), as shown in Fig. 1(a). MRI measurements were performed with spatial encoding of $M = 16$ in Eq. 11 and 12. A set of 512 data sampled at 1600Hz is used in the chemical-shift analysis. The chemical-shift spectrum obtained by the ordinary FT is Fig. 1(c). Using the fact that the spectrum of exponentially decaying sinusoids drops the magnitude down to a half of the peak at $\omega = \omega_0 + a$, if the envelope decays with e^{-at}, poles for each chemical-shift component, i.e. CH_3-, -CH_2-, and -OH, are determined. The CZT contour is thus determined as shown in Fig. 1(b). The spectrum sharpening gained by the CZT is shown in Fig. 1(d). Nine pictures of the reconstructed images in Fig. 2, in which frequency increases from left to right, then from top to bottom, show the tubes containing only methanol, those of ethanol, and both combined, as frequency increases. The reconstructed images by the FT method in Fig. 2(a) do not distinctly separate two types of alcohol due to the broad spectral lines. The CZT significantly improves the separation among chemical-shift spectral lines, resulting in much more distinct images as shown in Fig. 2(b).

The projection data for optical CT were measured by using a He-Ne laser beam modulated with a chopper as a light source, and a differential detector which consists of two sets of a collimator/ photodiode pair. The object is mechanically moved across the laser beam to obtain the projection profile. The total of 128 data spaced at 0.5mm is recorded. The object is rotated by 10° after each scan. Three metal rods of different shape; circular, triangular and rectangular, are immersed in a milky translucent liquid. Using 18 projections of 10° apart, the image is reconstructed by the standard FBP method [3], as shown in Fig. 3(a). Filtering is done in the frequency domain. Then, the CZT is used to convert the filtered data in the frequency domain back to the data for back-projection. Since the measurements are done by a thin scanning beam, a moderate CZT, in which the contour is chosen close to the FT contour, is used. The result is shown in Fig. 3(b).

Conclusion

The applications of the chirp z-transform to CT are discussed for two important modalities of CT, MRI and optical CT. In the case of MRI, the CZT is extremely effective as FID signals are basically decaying oscillation. As far as data acquisition is terminated when signals diminish and avoid to take in unnecessary noise, the method is

immune to noise. In optical CT, the CZT automatically cancels the smearing introduced by the point spread function of the measurement system. The concept does extend to other types of CT's such as X-ray CT. This is particularly effective when a flat beam as opposed to a single beam is used along with the array of multiple detectors.

References

1. T.R. Brown et. al. "NMR chemical shift imaging in three dimensions," Proc. Nat. Acad. Sci. vol. 78, pp. 3523-3526, 1982.
2. T.N. Ma and K. Takaya, "High- Resolution NMR Chemical- Shift Imaging with Reconstruction by the Chirp z-Transform," IEEE trans. on Med. Imag. vol. 9, No. 2, pp. 190-201, 1990.
3. M. Kitama et. al. "Tomographic imaging of biological body with light - Basic study on its feasibility," Proc. 29th Conf. Jap. Soc. of Med. Elec. and Bio. Eng. p. 510, 1990.

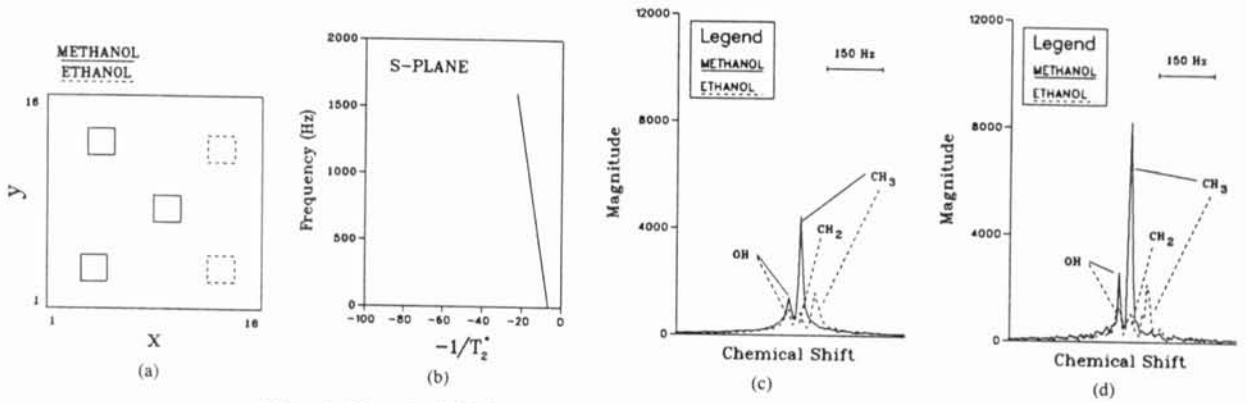

Fig. 1 Chemical-shift spectra and the Chirp-z transform contour

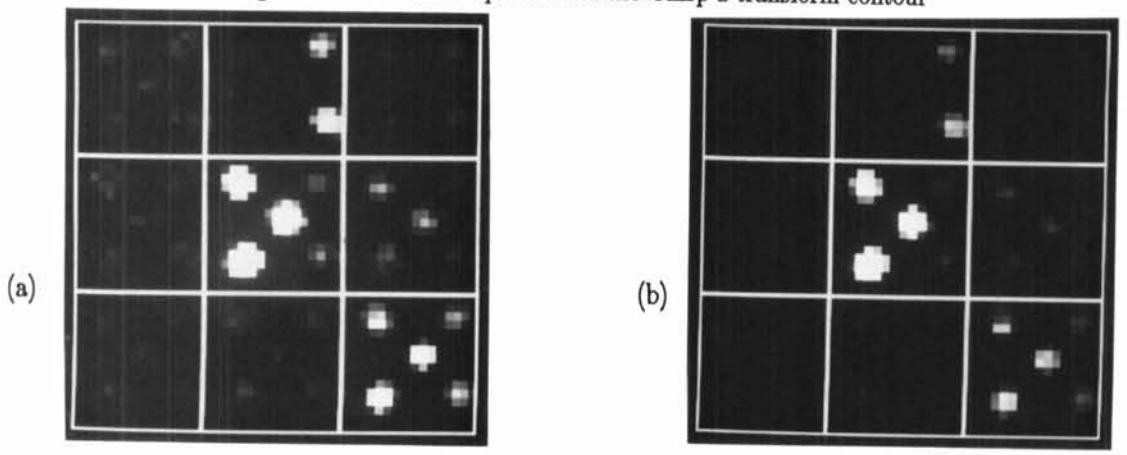

Fig. 2 Chemical-shift images reconstructed by FT and CZT

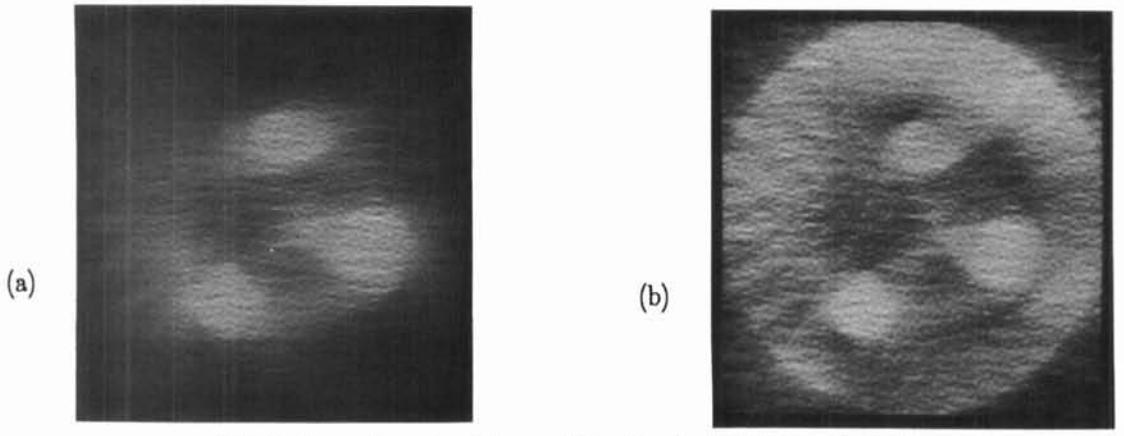

Fig. 3 Correction of point spread function by CZT for optical CT